AFRL-RV-PS-
TR-2015-0165

AFRL-RV-PS-
TR-2015-0165

ESTIMATING SOLAR PROTON FLUX AT LEO FROM A GEOMAGNETIC CUTOFF MODEL

Richard S. Selesnick, et al.

14 July 2015

Technical Report

AIR FORCE RESEARCH LABORATORY
Space Vehicles Directorate
3550 Aberdeen Ave SE
AIR FORCE MATERIEL COMMAND
KIRTLAND AIR FORCE BASE, NM 87117-5776

DTIC COPY

NOTICE AND SIGNATURE PAGE

Using Government drawings, specifications, or other data included in this document for any purpose other than Government procurement does not in any way obligate the U.S. Government. The fact that the Government formulated or supplied the drawings, specifications, or other data does not license the holder or any other person or corporation; or convey any rights or permission to manufacture, use, or sell any patented invention that may relate to them.

This report was cleared for public release by the 377 ABW Public Affairs Office and is available to the general public, including foreign nationals. Copies may be obtained from the Defense Technical Information Center (DTIC) (http://www.dtic.mil).

AFRL-RV-PS-TR-2015-0165 HAS BEEN REVIEWED AND IS APPROVED FOR PUBLICATION IN ACCORDANCE WITH ASSIGNED DISTRIBUTION STATEMENT.

//SIGNED//	//SIGNED//
Adrian Wheelock	Glenn M. Vaughan, Colonel, USAF
Project Manager, AFRL/RVBXR	Chief, Battlespace Environment Division

This report is published in the interest of scientific and technical information exchange, and its publication does not constitute the Government's approval or disapproval of its ideas or findings.

REPORT DOCUMENTATION PAGE

Form Approved
OMB No. 0704-0188

1. REPORT DATE *(DD-MM-YYYY)*	**2. REPORT TYPE**	**3. DATES COVERED** *(From - To)*
14-07-2015	Technical Report	07 Oct 2013 – 14 Jul 2015

4. TITLE AND SUBTITLE
Estimating Solar Proton Flux at LEO From a Geomagnetic Cutoff Model

5a. CONTRACT NUMBER

5b. GRANT NUMBER

5c. PROGRAM ELEMENT NUMBER
62601F

6. AUTHOR(S)
Richard S. Selesnick, S. Young, and L. Winter

5d. PROJECT NUMBER
1010

5e. TASK NUMBER
PPM00004260

5f. WORK UNIT NUMBER
EF004414

7. PERFORMING ORGANIZATION NAME(S) AND ADDRESS(ES)
Air Force Research Laboratory
Space Vehicles Directorate
3550 Aberdeen Avenue SE
Kirtland AFB, NM 87117-5776

8. PERFORMING ORGANIZATION REPORT NUMBER
AFRL-RV-PS-TR-2015-0165

9. SPONSORING / MONITORING AGENCY NAME(S) AND ADDRESS(ES)

10. SPONSOR/MONITOR'S ACRONYM(S)
AFRL/RVBXR

11. SPONSOR/MONITOR'S REPORT NUMBER(S)

12. DISTRIBUTION / AVAILABILITY STATEMENT
Approved for public release; distribution is unlimited. (377ABW-2015-0538 dtd 30 Jun 2015)

13. SUPPLEMENTARY NOTES

14. ABSTRACT

This report describes a method for predicting proton flux in low earth orbit (LEO) during a solar proton event (SPE). In particular, integral fluxes of >5 and >30 MeV protons are required, though it can be applied equally to other energy ranges. The method depends on a geomagnetic cutoff model, proton measurements from a geosynchronous (GEO) GOES satellite, and the geomagnetic Kp index. Its limitations and statistical accuracy are also described. The recommended cutoff model is empirical. Its results are also compared to the theoretical model of Smart and Shea.

15. SUBJECT TERMS
Geomagnetic cutoff; empirical cutoff model; solar energetic protons; low earth orbit

16. SECURITY CLASSIFICATION OF:			**17. LIMITATION OF ABSTRACT**	**18. NUMBER OF PAGES**	**19a. NAME OF RESPONSIBLE PERSON**
a. REPORT	**b. ABSTRACT**	**c. THIS PAGE**			Adrian Wheelock
Unclassified	Unclassified	Unclassified	Unlimited	24	**19b. TELEPHONE NUMBER** *(include area code)*

Standard Form 298 (Rev. 8-98)
Prescribed by ANSI Std. 239.18

This page is intentionally left blank.

Table of Contents

List of Figures

Estimating solar proton flux at LEO from a geomagnetic cutoff model

R. Selesnick, S. Young, L. Winter

July 14, 2015

1 Introduction

This report describes a method for predicting proton flux in low earth orbit (LEO) during a solar proton event (SPE). In particular, integral fluxes of > 5 and > 30 MeV protons are required, though it can be applied equally to other energy ranges. The method depends on a geomagnetic cutoff model, proton measurements from a geosynchronous (GEO) GOES satellite, and the geomagnetic Kp index. Its limitations and statistical accuracy are also described. The recommended cutoff model is empirical. Its results are also compared to the theoretical model of Smart and Shea.

2 Background

Empirical and theoretical models of geomagnetic cutoffs are available. Empirical models are generally simpler and easier to apply. Therefore, if they are of similar accuracy, they are preferable for practical application.

3 Method, assumptions, and procedures

For each location in LEO the model proton cutoff energy is determined using Kp. Then the differential proton flux measured at GOES is integrated over the energy range of interest, but excluding energies below cutoff, to determine the integral flux at LEO.

Cutoff kinetic energy E_c is obtained from proton rigidity $R = pc/e$ where p is momentum, $p^2c^2 = E(E + 2mc^2)$, E is kinetic energy, m is the proton rest mass, c is the speed of light, and e is the elementary charge. The cutoff rigidity in GV is:

$$R_c = 17.635 \cos^4(\lambda + 0.38K_{ps} + 0.06K_{ps}^2) - 0.468 \tag{1}$$

where K_{ps} is the shifted Kp, the value of Kp from 3 hours earlier. The invariant latitude of the LEO location is related to the magnetic L shell by $\cos^2 \lambda = 1/L$ where L is computed in the IGRF magnetic field model. If equation (1) gives $R_c < 0$ then $E_c = 0$, as appropriate to high invariant latitudes. For low latitudes ($\lambda \lesssim 50^\circ$) all protons of interest are below cutoff.

Equation (1) is a combination of empirical relationships, between R_c and λ during geomagnetically quiet times [1], and between λ and K_{ps} at fixed E_c [2], obtained from LEO observations of

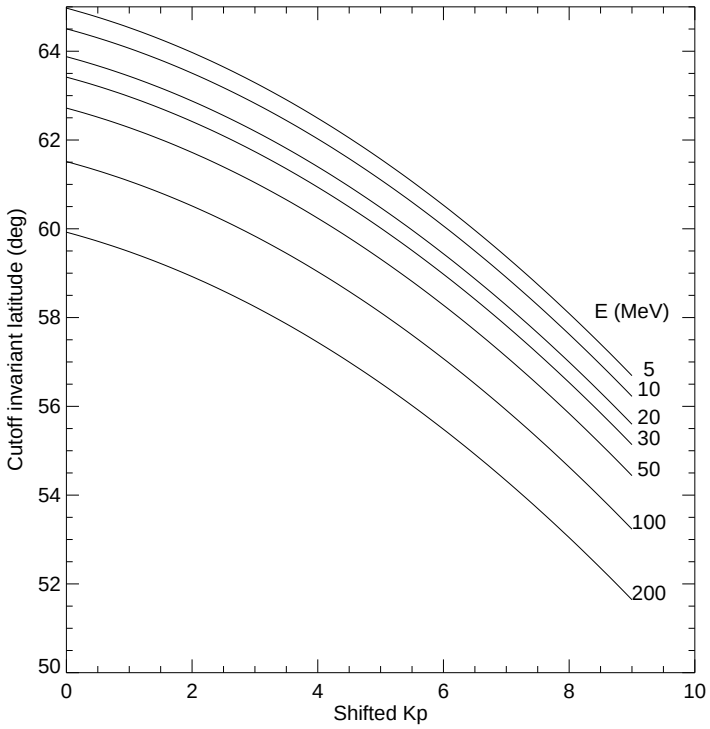

Figure 1: Cutoff λ versus shifted Kp for various protons energies from equation (1).

proton cutoffs. The dependence of cutoff invariant latitude on proton energy and shifted Kp from equation (1) is shown in Figure 1. An alternate formulation to equation (1) was also provided. It replaces the constants 17.635 by 15.062 and -0.468 by -0.363 [1]. The validation method described below shows the first formulation to be marginally preferable for the present application. However, the alternate formulation is preferred by the original authors (Mewaldt, R.A., private communication, 2013) and could replace equation (1) with negligible impact.

The GOES data [3] provide measurements of proton flux in a few fixed-width energy channels. A simple procedure is used to convert them to a continuous differential energy spectrum: For each channel, the measurement is assumed to provide the differential flux at the geometric mean limits of the channel. In between these mean energies the differential flux is obtained by power law interpolation, that is, by assuming a power-law energy spectrum connecting the fluxes at the channel mean energies. For energies outside the range of the data, power-law extrapolation is used from the two lowest or highest energy channels.

The method of determining the GOES proton spectrum is illustrated in Figure 2. It shows data points at the geometric mean energy of each differential channel, connected by power law segments. This defines the differential intensity (or flux) at each energy. A more sophisticated method could be used to determine the GOES spectrum, but this seems unwarranted given the uncertainties involved.

To predict the integral proton flux above a given energy E_0 (e.g., 5 or 30 MeV) at LEO, the GOES differential spectrum is integrated above the maximum of E_0 and E_c. Direct mapping of measured GOES energy spectra to LEO is justified by the assumption that interplanetary solar protons are isotropic. Liouville's theorem then states that flux is uniform along dynamical proton

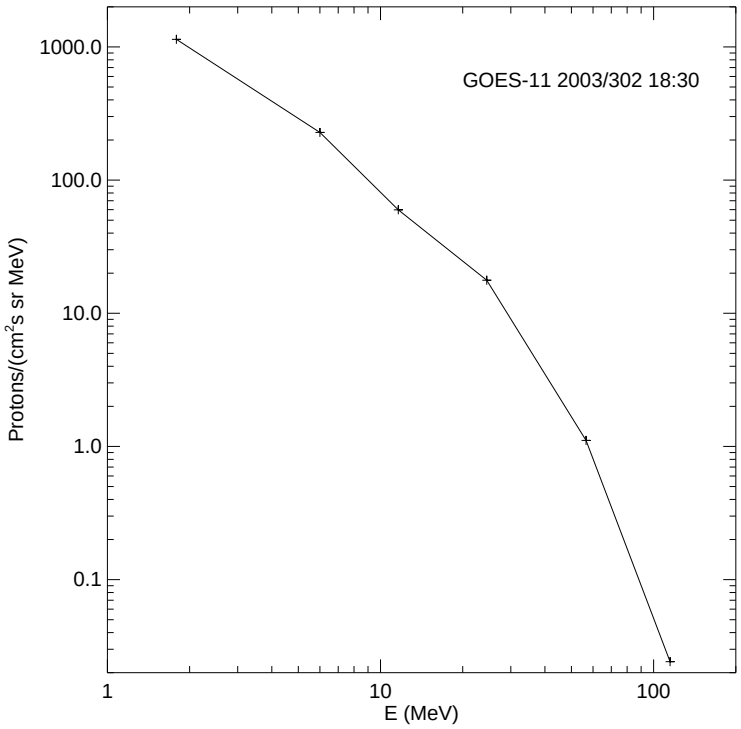

Figure 2: A sample proton differential energy spectrum from GOES-11.

paths reaching GEO or LEO from interplanetary space. The validity of the assumption is subject to limitations described below.

4 Results and discussion

4.1 Empirical cutoff model

The method was tested by comparing its results to data taken by the PET and MAST instruments on the SAMPEX satellite during the October and November 2003 SPEs. Close substitutes for the > 5 and > 30 MeV energy ranges are available respectively from MAST/M12 data, for 5 to 12 MeV protons, and the PET data for 27.4 to 53.0 MeV protons [4]. The former is available with 96 s resolution and the latter with 6 s resolution. Energy spectra from GOES-11 were integrated over each of these energy ranges for direct comparison to the data. The GOES data are available with 1-min resolution. All of the available data points between the start of Oct 26 (day 299) and the end of Nov 7 (day 311), 2003, are shown in Figure 3.

For the upper energy range the GOES flux is generally higher than the SAMPEX flux and the reverse is true for the lower energy range. It is unclear whether these discrepancies are due to systematic errors in the data, or to real differences between LEO and GEO, or a combination of both. (Real differences could result from imperfect access to the of solar protons to the low-altitude polar cap, effecting mostly the higher energy range, or cutoff effects at GEO, effecting mostly the lower energy range.) The close correspondence of the flux variations at LEO and GEO for each energy range shows that equivalent proton energies were being measured.

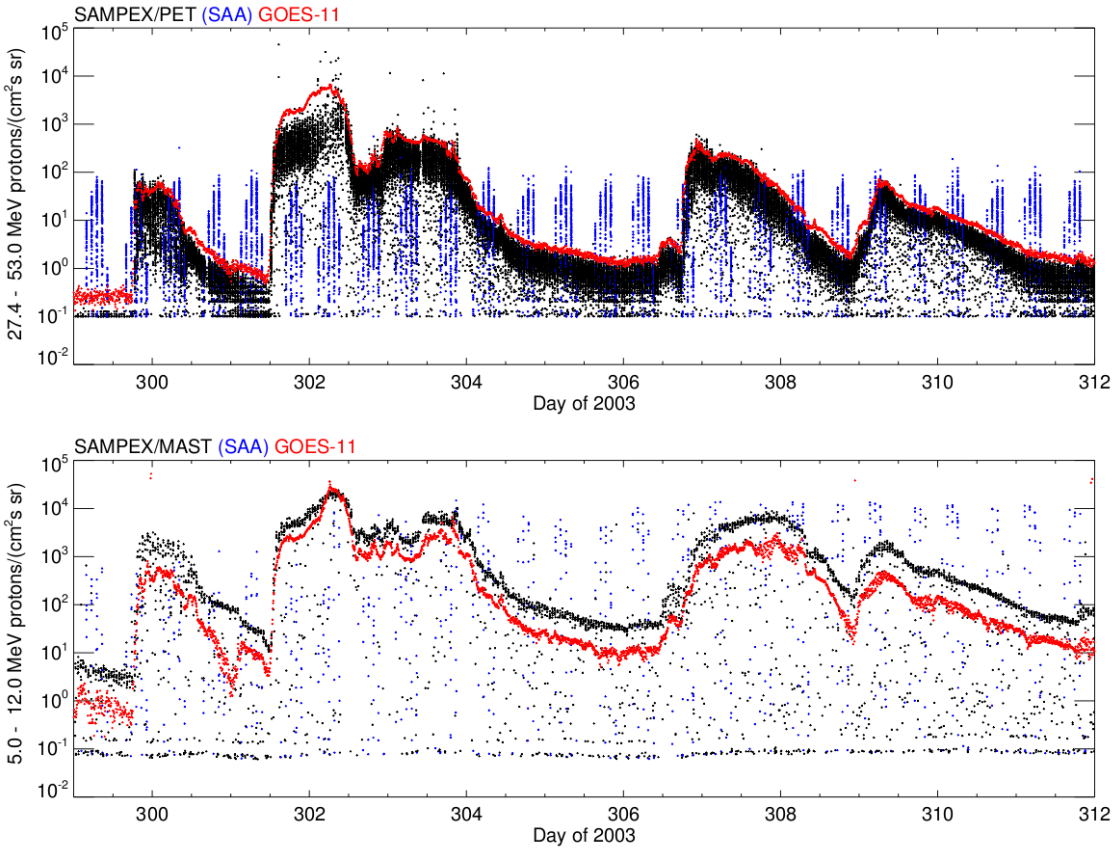

Figure 3: Proton flux data versus time from SAMPEX (black, or blue in the SAA) and GOES-11 (red) during the Oct/Nov 2003 SPEs.

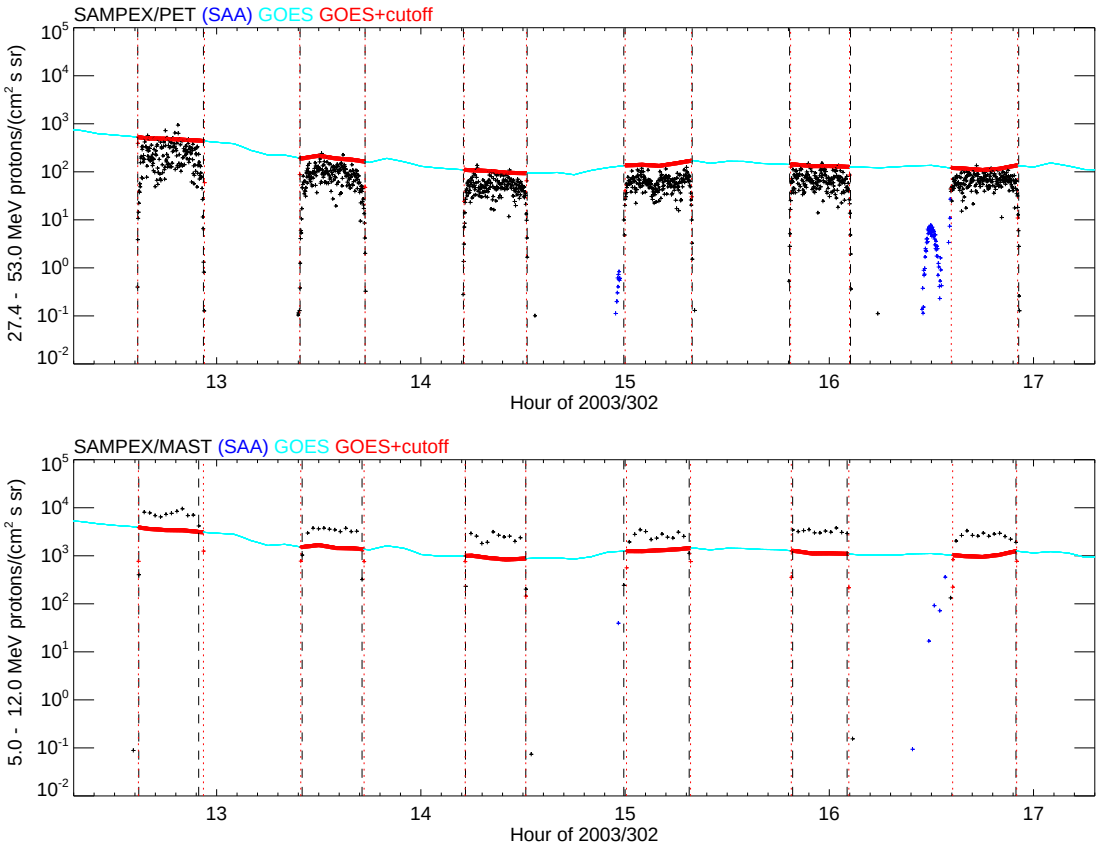

Figure 4: Proton flux from SAMPEX and GOES versus time from 2003 day 302. *GOES data are shown with/without the cutoff model applied (red/cyan). Vertical lines show cutoffs identified from SAMPEX data (dashed black) and from GOES data with the cutoff model (dotted red).*

The wide spread in the SAMPEX data for the higher energy range is a result of statistical fluctuations, with only zero to a few protons per 6-s interval. This is because high fluxes cause significant instrumental deadtime. Corrections for deadtime are uncertain at the highest fluxes, as is particularly evident in early day 302. Trapped protons in the South Atlantic Anomaly (SAA) are encountered periodically by SAMPEX due to Earth's rotation.

A closer view of data from the second half of day 302 is shown in Figure 4. All SAMPEX data are included. The GOES data were interpolated linearly in time from 5-min averages to the times of the SAMPEX data points. They are shown with and without application of the cutoff model. Cutoff times determined from the SAMPEX data and the GOES data with model cutoff are shown in the Figure by vertical dashed and dotted lines respectively. The time of each cutoff was determined as the first and last points above a background flux level, and not in the SAA, during each polar pass. A background level of 1 proton/(cm^{2}s sr) was chosen; results are generally insensitive to this choice. Cutoff determinations were discarded if an adjacent data point was in the SAA or if the maximum flux during the full polar pass was below a threshold value of 3 or 100 proton/(cm^{2}s sr), for the higher or lower energy range respectively.

The times of each cutoff determined from the data correspond to values of λ along the SAMPEX orbit. These cutoff invariant latitudes from each energy range are shown as a function of shifted Kp for the entire data interval in Figure 5. Those from the GOES data closely follow a smooth curve established by the cutoff model, with small deviations resulting only from the 6-s time resolution of the SAMPEX data, which corresponds to an uncertainty of $\sim$0.2° invariant latitude. Those

from the SAMPEX data show additional scatter that likely results from geomagnetic variations not described by the simple Kp index. Scatter in lower energy range SAMPEX results is also increased by their 96-s time resolution, corresponding to $\sim 3^\circ$ invariant latitude uncertainty.

Two numbers describe the accuracy of the cutoff model. First, the mean difference between the observed (SAMPEX) and model (GOES) cutoffs shows the accuracy on average. It is 0.01° and -0.63° for the higher and lower energy ranges, respectively, showing a good average fit of data to model. The scatter of the observed cutoffs away from the model is described by the standard deviation or root-mean-square (RMS) values of 1.51° and 2.16°, obtained by subtracting the mean difference from each difference value, then squaring, taking the mean of the resulting values, and finally the square root. To avoid undue influence from outliers, differences greater than 5° have been excluded from the mean and RMS values. These result mainly from misidentification of SAA trapped protons, causing low observed cutoffs, some of which are clearly evident in the lower energy range. Their exclusion is therefore justified. The RMS value in the lower energy range includes the effect of low time resolution in those data. If higher time resolution were available the RMS value would likely be comparable to the value of 1.51° obtained for the higher energy range.

4.2 Smart and Shea cutoff model

More sophisticated methods, compared to the simple empirical model of equation (1), have been developed for obtaining cutoffs. They consist of numerical computations of test-particle motion in models of the combined geomagnetic and magnetospheric magnetic fields, to determine whether the particles have access to interplanetary space. However, these methods have not yet achieved sufficient accuracy to replace an empirical model in practical applications. This is now demonstrated using the method of Smart and Shea [5]. It uses interpolation in a grid of precomputed cutoffs from the combined IGRF and T89 field m odels. It therefore has the advantage of being efficient to run and is easily implemented.

The method provides several cutoff values at each location: effective, lower, and upper cutoff energies for the vertical, east, and west directions. The SAMPEX detectors point mostly to the zenith, so the vertical cutoffs are most appropriate (though fields-of-view are relatively wide; 101° and 58° full angle for MAST and PET respectively). At low altitude, directional (east-west) effects on cutoffs are small, but they become much more significant at higher altitude.

Results equivalent to Figure 5, but using the Smart and Shea method with the effective ver-tical cutoff, are shown in Figure 6 (they are again shown versus shifted Kp, but the cutoffs are determined from unshifted Kp in this case). It is seen that the cutoff locations are offset poleward of the observed values by, on average, 1.3° and 1.42° for the higher and lower energy ranges respectively. Even correcting for these offsets, the RMS values show a somewhat worse agreement with the observed values than do those of the empirical cutoff model. Although the observed and model values from the Smart and Shea method show a similar degree of scatter, it is evident from the RMS values this the scatter is uncorrelated from point to point. The scatter from the Smart and Shea model results mostly from variations in the local time and the hemisphere (north/south) of the satellite location, but such systematic effects are not apparent in the observed cutoff values.

Exclusion of outliers biases the results of Figure 6. To correct for this the model cutoffs have been offset by constant factors of 1.8° and 3.0°, for higher and lower energies respectively, that reduce the mean differences to nearly zero. These offsets were obtained by trial and error to achieve the near zero mean differences. They represent the true errors of the Smart and Shea method, rather than the mean differences from Figure 6. Results are shown in Figure 7. Now the RMS values have changed somewhat but are still worse than from the empirical model.

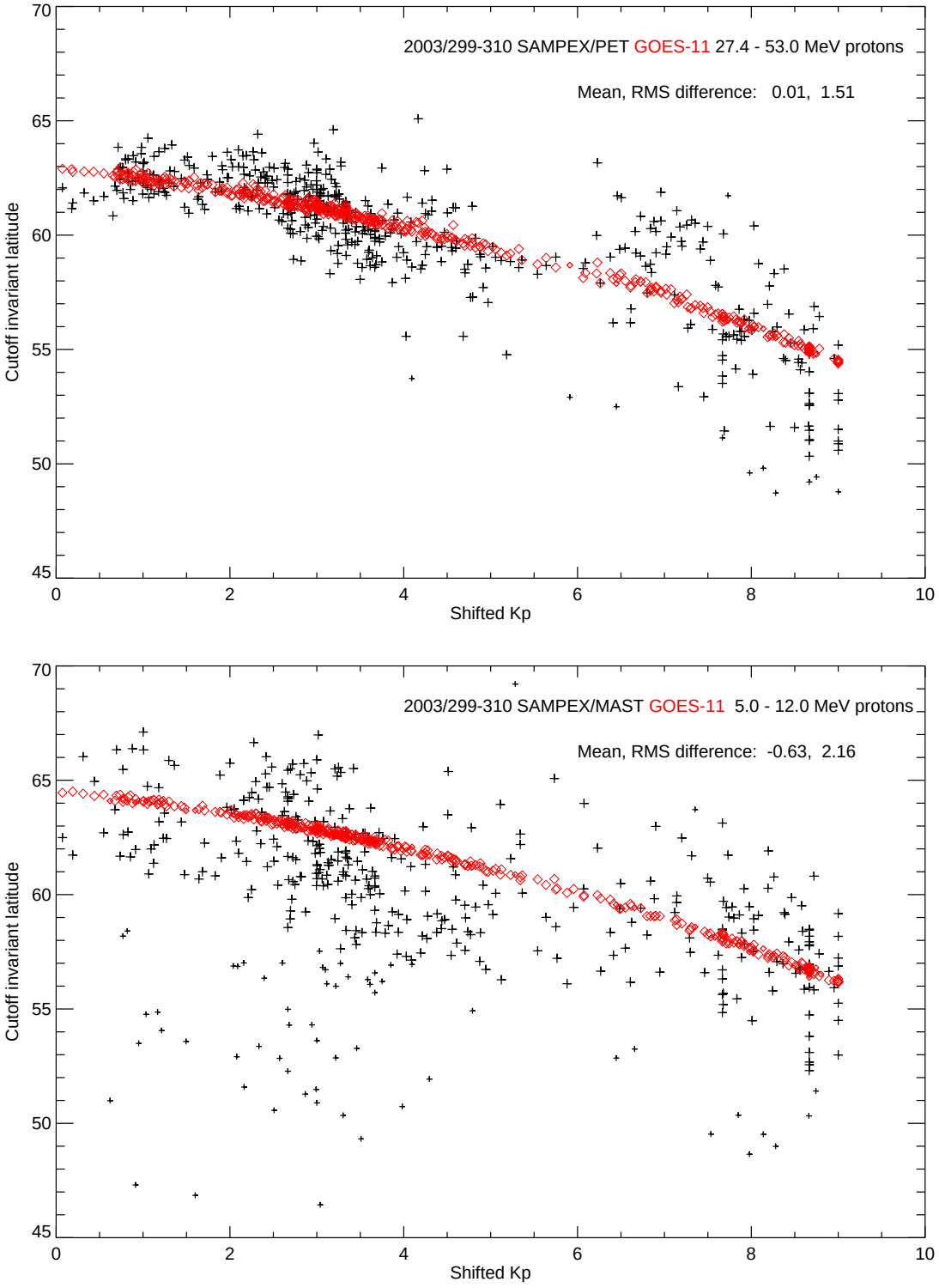

Figure 5: Identified cutoff λ versus shifted Kp from SAMPEX data (black) and from GOES data with the cutoff model (red). *Smaller symbols are outliers not used in computing the mean and RMS differences.*

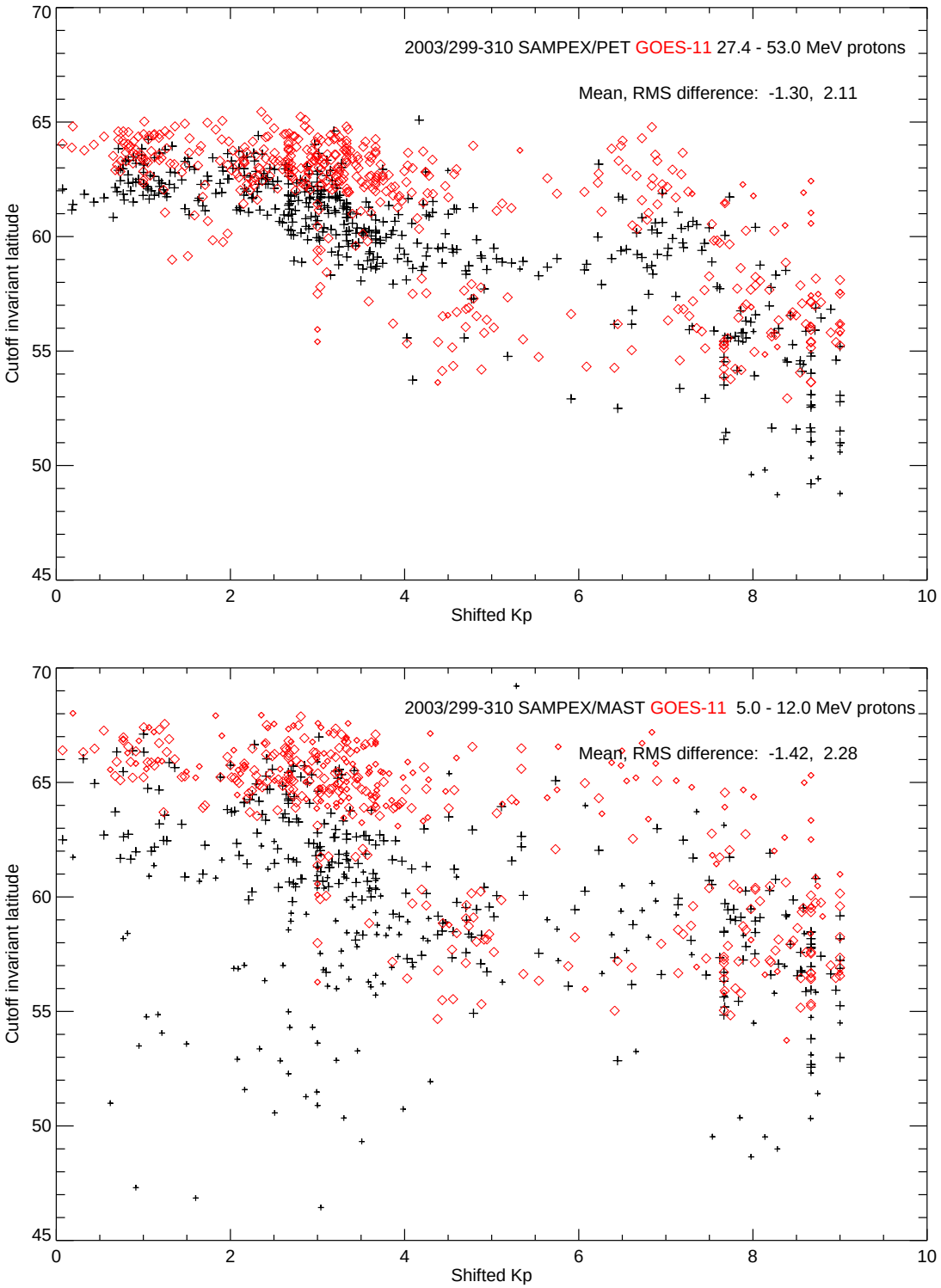

Figure 6: Similar to Figure 5, but using the Smart and Shea effective vertical cutoff model.

The method for determining observed cutoffs was to place them at the lowest invariant latitudes of observed polar protons. This suggests that the Smart and Shea lower cutoff should perhaps be used instead of the effective cutoff, and this may account for the poleward offsets described above. Results using the lower vertical cutoffs instead of the effective vertical cutoffs, with no extra offsets, are shown in Figure 8. The poleward offsets are in fact reduced relative to the effective cutoffs, particularly at the higher energy range, but the reductions are insufficient and the empirical model is still superior.

The lower and upper cutoffs in the Smart and Shea method describe the effects of the penumbra and simple shadow cones (using nomenclature from Stormer theory of particle motion in a dipole magnetic field [6]), that result from particles trajectories intersecting the solid Earth. The model also includes a transparency function to describe the fraction of trajectories that have access to any location in between the lower and upper cutoffs. This suggests that the simple empirical cutoff model cannot describe the full variation in proton flux with invariant latitude. In fact, close inspection of Figure 4 shows that the cutoff is usually more gradual than predicted by the model. This effect is illustrated more accurately in Figure 9. It shows the average polar flux, normalized to the mean value from $\lambda > 65^\circ$, as a function of difference in λ from the measured cutoff location. The flux is seen to increase from $\sim$0.25 of its full polar value at cutoff, to its full value at $\sim 3^\circ$ above cutoff, on average, nearly independent of energy. (The lower energy range of the MAST data is not useful here because of its poor time resolution. It has been replaced by 19 to 24 MeV protons from PET for which the 6-sec resolution is available.) This invariant latitude range of $\sim 3^\circ$ over which the cutoff occurs is a measure of the difference between the lower and upper cutoffs, using the Smart and Shea nomenclature, but is wider than the range predicted by the model.

4.3 Other solar proton events

The results described above were for a sequence of SPEs in 2003 (Figure 3). Similar results from other SPEs during 1998 to 2005 are shown in Figure 10, from the upper energy range of the SAMPEX data only. Measured cutoffs for the separate events are distinguished by color. They show that there are systematic variations between events, with mean differences from the empirical model cutoffs changing from event to event by $\sim 1^\circ$. Averaging over all events, the empirical model matches the data approximately as it did during the 2003 events. It is not necessary to retest the Smart and Shea model because it depends only on Kp and would also perform as it did during 2003.

The cause of the systematic variations between events is unclear, but again must be geomagnetic effects unrelated (or partly unrelated) to Kp. These can be caused by variations in factors such as the ring current, solar wind dynamic pressure, and interplanetary magnetic field. Model cutoffs have been computed from test-particle simulations using complex magnetic field models that include these factors as input parameters [8]. They show a close agreement with observed cutoffs, except for a similar poleward shift as obtained from the Smart and Shea model (Kress, B.T., private communication, 2013). It is likely that an empirical model could be constructed to also include these factors and provide more accurate cutoff predictions than the simple model of equation (1), but such an empirical model is not available.

Proton intensity versus time from the start of an SPE on 20 January 2005 is shown in Figure 11, with the same format as Figure 4. The start of the event near hour 7 occurred earlier in the GOES data than in the SAMPEX data, showing that LEO proton flux is not always directly related to GEO

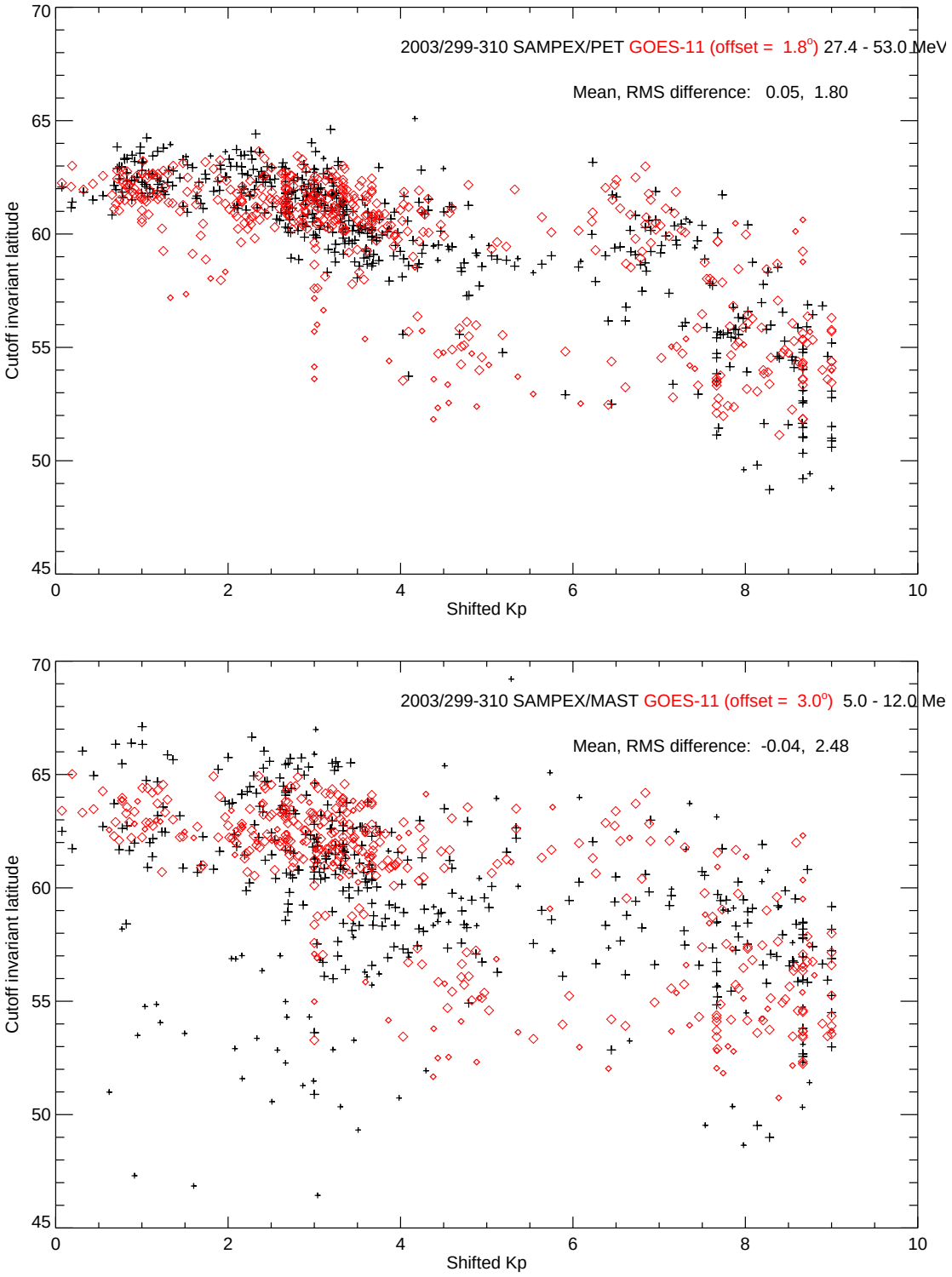

Figure 7: Similar to Figure 6, but cutoffs identified from GOES data with the Smart and Shea effective vertical cutoff model have been shifted equatorward by 1.8 and 3°.

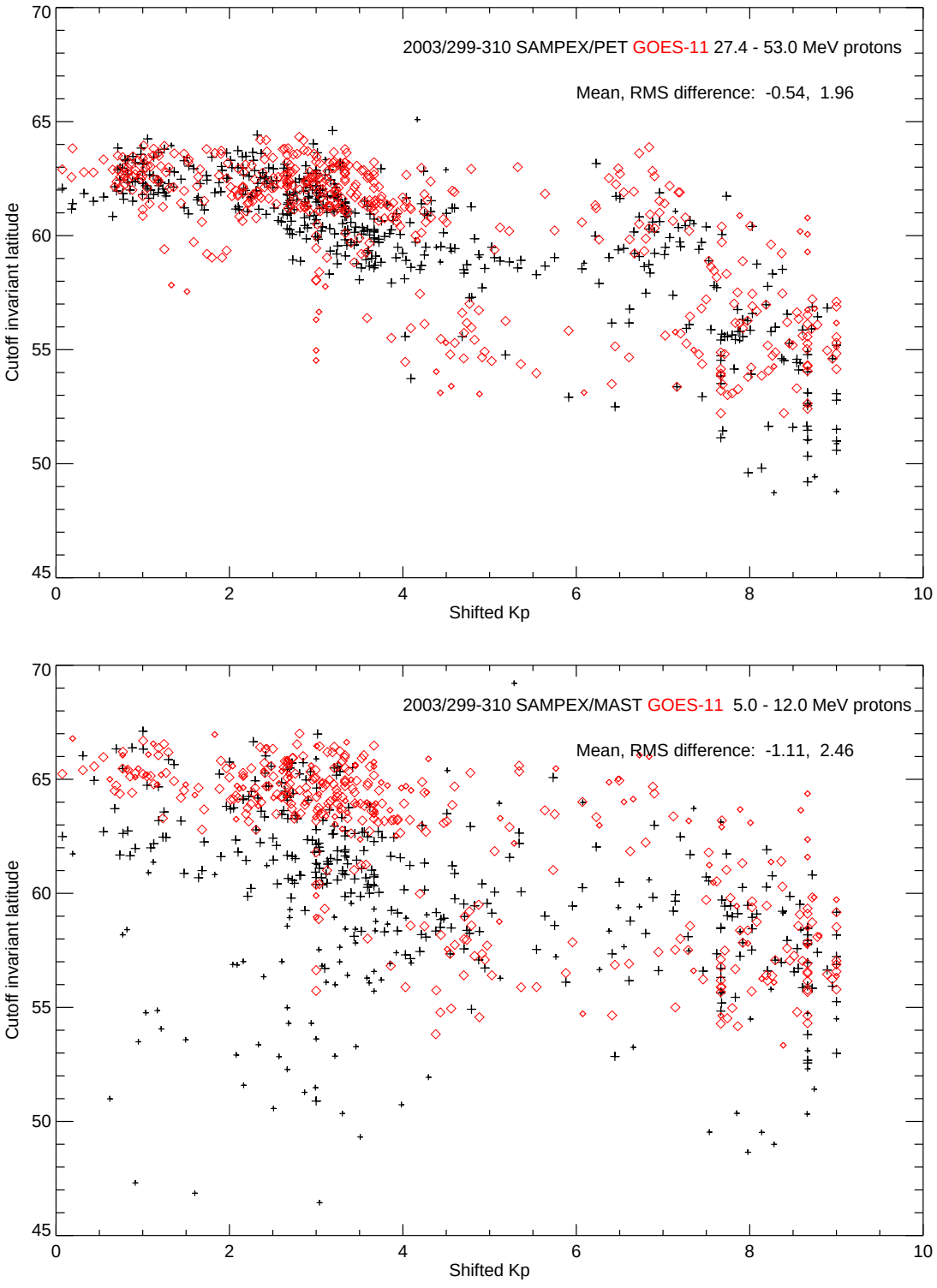

Figure 8: Similar to Figure 6, but with the Smart and Shea lower vertical cutoff model.

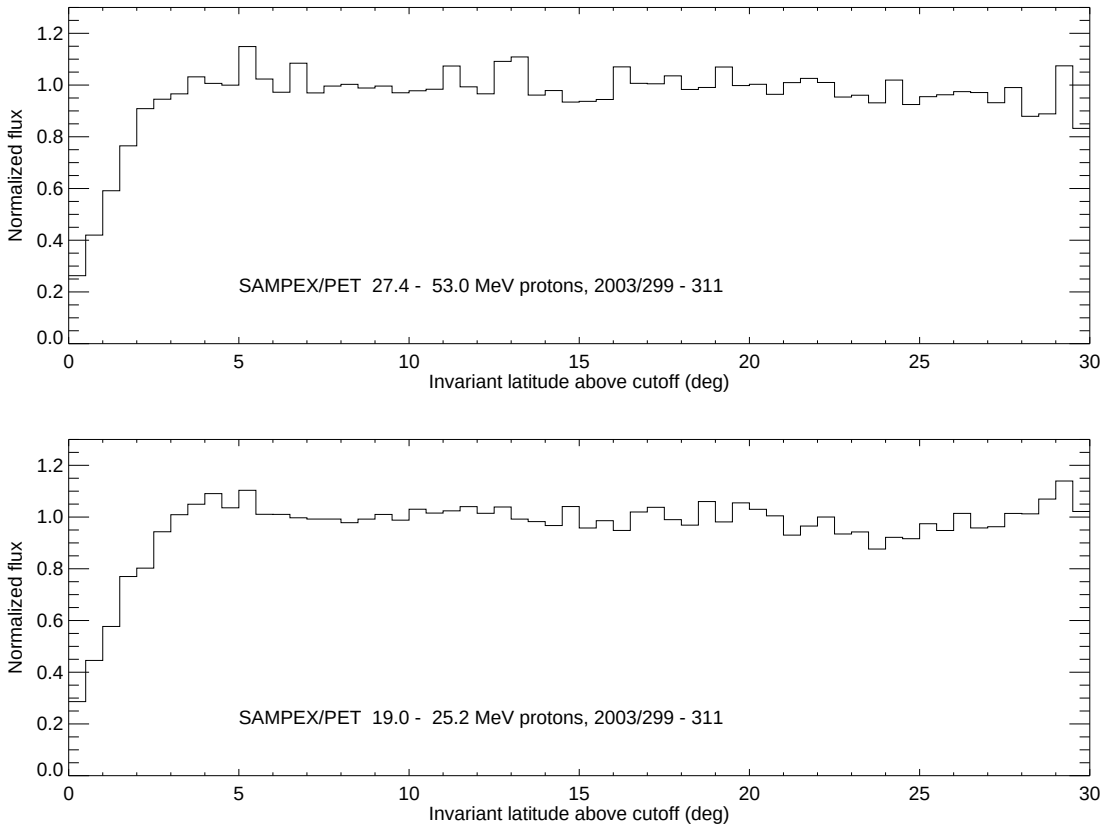

Figure 9: Averaged normalized polar cap proton flux from SAMPEX data, as a function of difference in λ from each identified cutoff (cutoff λ is at zero, λ above cutoff increases poleward).

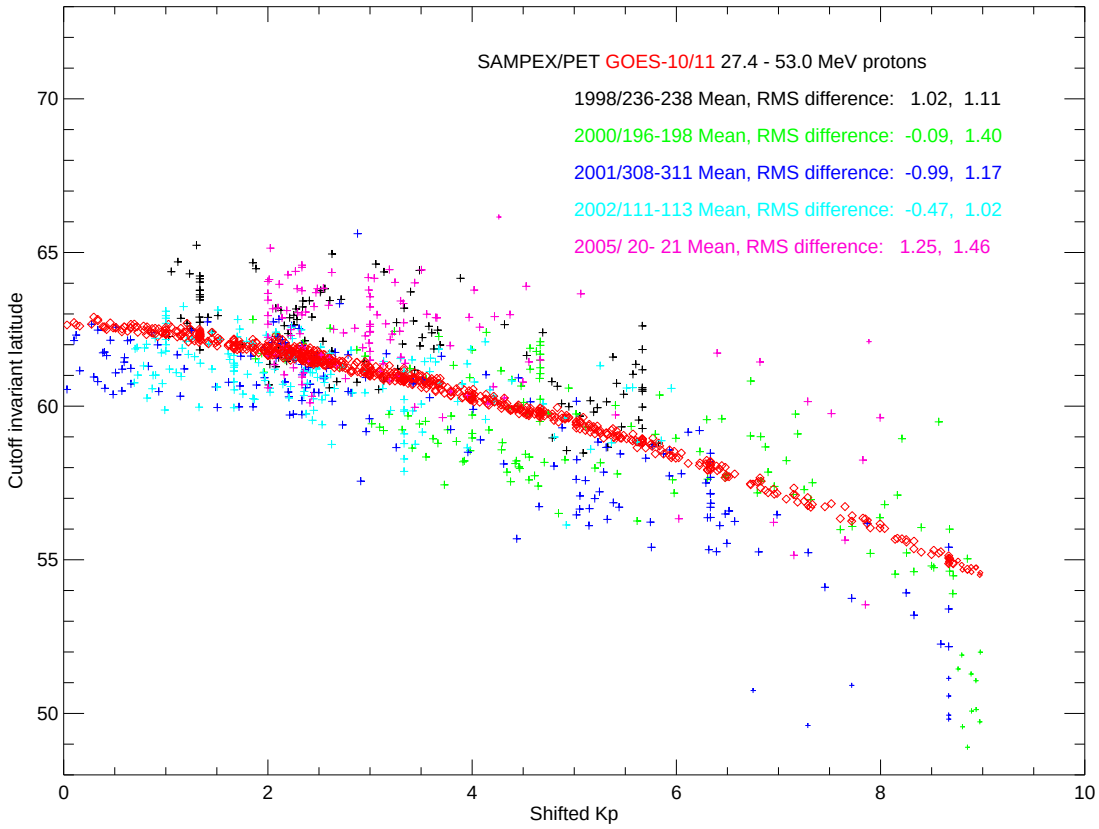

Figure 10: Similar to Figure 5 but for SPEs during 1998 to 2005 as indicated by the color coding and for the upper energy range only.
Empirical model cutoffs (red) were derived from the equation (1) and GOES-10 or GOES-11 data as available. Mean and RMS differences from the model cutoffs are shown separately for each SPE (cutoffs below 52 ◦ were also excluded as outliers in this case, due to misidentified SAA protons).

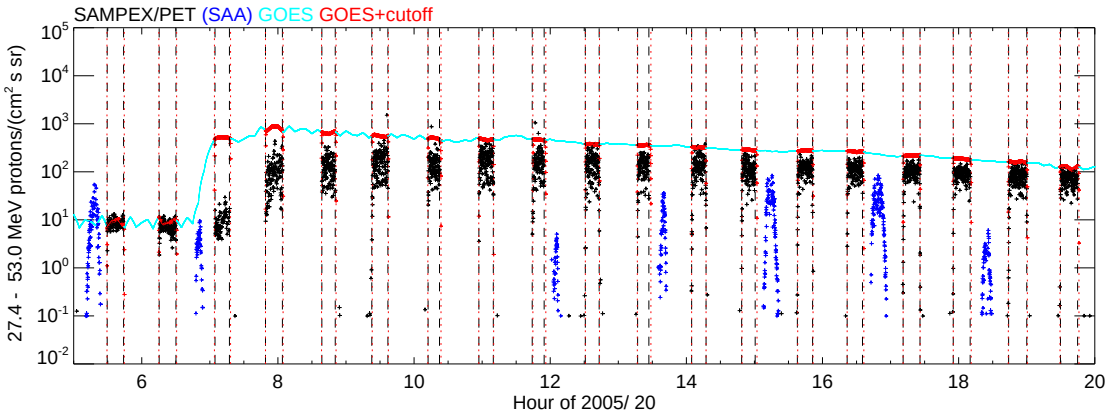

Figure 11: Similar to Figure 4 but with data from an SPE in January 2005.

fluxes. This was probably a result of proton anisotropy at the start of the event. Note that prior to hour 7 the SAMPEX and GOES fluxes were in good agreement and nearly a full day after the start of the SPE was required to approach agreement again. Such discrepancies are frequently observed when an SPE begins suddenly (these are cases in which Earth is magnetically well connected to the source region).

5 Conclusions

The main factor in predicting the flux at LEO from measurements at GEO is in modeling the cutoff. The empirical cutoff model was shown to be accurate on average, but with point-to-point fluctuations described by a standard deviation of $\sim$1.5°invariant latitude, and with systematic deviations between SPEs of $\sim$1°. The cause of the fluctuations and systematic effects is unknown, but likely a combination of geomagnetic and interplanetary factors not included in the model. However, the empirical model is superior to the Smart and Shea model both in mean accuracy and standard deviation. It is also simpler to apply, though both are relatively simple.

In addition to the cutoff model, errors can be introduced by flux differences between GEO and polar LEO. Some of the differences are known to be caused by incomplete proton access to the polar cap [7] and some by cutoff effects at GEO [9]. The latter can be minimized by choosing a GOES satellite near midnight and a GOES proton detector facing west, for which cutoffs are lowest. If suitable GOES data are unavailable then data from an interplanetary platform such as ACE could be used instead.

It is also possible that there are systematic instrumental errors that cause differences in measured flux between LEO and GEO. These are easily confused with true differences caused by geomagnetic access effects. Usually the differences are within a factor $\sim$2 (Figure 3), though may be much greater at the start of an event (Figure 11).

The simple cutoff model does not describe flux variations near cutoff that may be caused by penumbra, shadow cone, and east-west effects. It has not been established whether these are the only causes of such variations because they have not yet been fully modeled theoretically. However, empirical estimates of the average flux change near cutoff, as in Figure 9, could be used in combination with the empirical cutoff model.

The empirical model of equation (1) was validated using data from particle detectors pointing nearly at zenith, and therefore represents vertical cutoff. If instead fluxes are required in some other direction, or omnidirectional fluxes are required, then the model could be adjusted using basic Stormer theory [7]. However, in LEO the changes would be small relative to uncertainties in the model and therefore unnecessary. If the model were applied at higher altitude such changes could be significant. However, other model errors will certainly also increase with altitude.

The empirical model of equation (1) was established using particle data taken during $\sim$1992-2003. In principle it should be time dependent due to the geomagnetic secular variation. Changes in the Earth's dipole moment could be included by scaling the first term on the right of equation (1), to which it is proportional. Changes in higher order moments cannot be included without new cutoff measurements. However, it is expected that any such changes will have a minimal effect over at least the next decade or two.

References

[1] Ogliore, R. C., et al. (2001), A Direct Measurement of the Geomagnetic Cutoff for Cosmic Rays at Space Station Latitudes, *Proceedings of ICRC 2001,* Hamburg, Germany.

[2] Neal, J. J., C. J. Rodger, and J. C. Green (2013), Empirical determination of solar proton access to the atmosphere: Impact on polar flight paths, *Space Weather, 11,* pp. 420–433, doi:10.1002/swe.20066.

[3] http://ngdc.noaa.gov/stp/satellite/goes/index.html, GOES Space Environment Monitor, accessed Dec 2013.

[4] http://www.srl.caltech.edu/sampex/DataCenter/data.html, MAST M12 from "6-second intensities - all instruments," PET 27.4 to 53 MeV protons contructed from the sum of channels 4 to 6 in "6-second H, He intensities from PET," accessed Dec 2013.

[5] Smart, D. F. , M. A. Shea, A. J. Tylka, and P. R. Boberg (2006), A geomagnetic cutoff rigidity interpolation tool: Accuracy verification and application to space weather, *Advances in Space Research, 37,* pp. 1206–1217.

[6] Rossi, B. and S. Olbert (1970), *Introduction to the Physics of Space,* McGraw-Hill.

[7] Morfill, G. E. and J. J. Quenby (1971), The entry of solar protons over the polar caps, *Planet. Space. Sci., 19*, pp. 1541–1577.

[8] Kress, B. T., C. J. Mertens, and M. Wiltberger (2010), Solar energetic particle cutoff variations during the 29–31 October 2003 geomagnetic storm, *Space Weather, 8,* S05001, doi:10.1029/2009SW000488.

[9] Kress B.T., J.V. Rodriguez, J.E. Mazur, and M. Engel (2013), Modeling solar proton access to geostationary spacecraft with geomagnetic cutoffs, *Advances in Space Research,* in press.

DISTRIBUTION LIST

DTIC/OCP
8725 John J. Kingman Rd, Suite 0944
Ft Belvoir, VA 22060-6218 1 cy

AFRL/RVIL
Kirtland AFB, NM 87117-5776 1 cy

Official Record Copy
AFRL/RVBXR/Adrian Wheelock 1 cy

This page is intentionally left blank.